ECS Transactions, 68 (1) 1383-1390 (2015)
10.1149/06801.1383ecst ©The Electrochemical Society

The Influence of Sulfur Poisoning and YSZ Substrate Orientation on Electrochemical Properties of Nickel Pattern Anodes

M. C. Doppler[a,b], J. Fleig[a], and A. K. Opitz[a,b]

[a] Vienna University of Technology, Institute of Chemical Technologies and Analytics, Getreidemarkt 9/164 Vienna, 1060, Austria
[b] Christian Doppler Laboratory for Interfaces in Metal-Supported Electrochemical Energy Converters, Getreidemarkt 9/164-EC Vienna, 1060, Austria

Micro-patterned Ni thin films with well-defined 2D-structures are useful to examine electrochemical reaction kinetics of SOFC anodes. In this work, an electrode preparation method is developed yielding stable Ni pattern electrodes on YSZ, which facilitate long term measurements. Moreover, these stable electrodes allowed investigating the effect of the YSZ substrate orientation on the polarization resistance and interface capacitance. Statistical analysis of data obtained from 3 different substrates revealed no significant difference in polarization resistances and no significant difference in interface capacitance between single crystalline substrates ($\alpha = 0.05$). Also, the effect of hydrogen sulfide on the polarization resistance was examined and the results are qualitatively equivalent to findings on cermet electrodes.

Introduction

Current state-of-the-art anodes for solid oxide fuel cell (SOFC) applications consist of a porous network of percolating nickel and yttria stabilized zirconia (YSZ) grains. This approach, while yielding excellent electrochemical performance, is rather impractical for kinetic studies aiming at a mechanistic understanding since gas phase transport and ionic transport can also contribute to electrode polarization and geometric data like triple phase boundary length are not easily accessible. To circumvent these obstacles, geometrically well-defined thin film electrodes, commonly referred to as pattern electrodes, are often employed (1-5). A potential issue related with pattern anodes is the morphological instability of the metallic Ni thin film on the oxidic YSZ electrolyte leading to changes of the electrode geometry during the measurements – e.g. due to pinhole formation. Owing to such alterations also the polarization resistance changes with time (6). Consequently, unambiguous identification of additional effects leading to changes in the polarization resistance is difficult. Thus, in the first part of the present study a method for obtaining long term stable Ni pattern anodes is introduced.

In literature, Ni pattern anode studies mostly employed (100) YSZ single crystal or polycrystalline YSZ substrates (6, 7). Rao et al. reported differences in polarization resistance and interface capacitance depending on the orientation of the substrate (8). This would mean that comparison of literature data obtained on different electrolyte substrates, as done by Bessler et al. (1), is not straightforwardly possible. However, the differences between the electrodes on differently oriented YSZ electrolytes in Ref. (3)

were rather small and additional influences on the polarization resistance, e.g. of impurities, may be the reason for observed differences. Hansen et al. reported scattering of polarization resistance values indicating that statistical analysis is necessary to verify the claims of Rao et al. (3, 8). The aim of the second part of this study is to provide the necessary statistical analysis.

Performance decrease of Ni/YSZ anodes due to sulfur impurities in the gas feed has already been studied extensively (9). There is, however, besides a theoretical modeling paper no study examining the effect of sulfur poisoning on Ni pattern anodes although it is possible to directly access the effect on triple phase boundary kinetics (10). In the third part this study therefore aims to close this knowledge gap by providing experimental data which can be used for further modeling the sulfur poisoning behavior of Ni pattern anodes.

Experimental

Three types of YSZ substrates were used: (100) and (111) 10×10×0.5 mm³ YSZ single crystals (9.5mol% Y_2O_3, one-sided polished, Crystec, GER) and a polycrystalline substrate. The latter was prepared from YSZ powder (TZ-8Y, TOSOH, JAP) by cold-isostatic pressing, sintering at 1550°C for 5h, cutting and polishing (last polishing step with 1µm diamond paste). On the unpolished side of the substrate the counter electrode was applied consisting of porous lanthanum strontium ferrite ($La_{0.6}Sr_{0.4}FeO_{3-\delta}$) with Pt paste as current collector.

Microelectrodes were prepared by depositing 1.2 µm Ni on the polished side of the substrate by magnetron sputtering and recrystallization of the film at 750°C for 18 hours in $2.4 \cdot 10^3 Pa$ H_2/ $3 \cdot 10^3 Pa$ H_2O/ balance Ar atmosphere. 800 nm thick Ni films lead to a porous layer after annealing under these conditions and were, despite their for impurity segregation more favorable volume to surface ratio, not used in this study. Photoresist (ma-N 1420 Negativ Photoresist, Micro Resist Technology GmbH, GER) was applied onto the film and photolithographically structured. Subsequently the sample was chemically etched with aqua regia until the final microelectrode structure was obtained.

Electrochemical measurements were performed in a the setup sketched in figure 1, which is described in detail elsewhere (11). Electrochemical measurements were conducted at 750°C in an atmosphere containing $2.4 \cdot 10^3 Pa$ H_2/ $3 \cdot 10^3 Pa$ H_2O/ balance Ar and sulfur poisoning experiments were done in $1 Pa$ H_2S/ $2.4 \cdot 10^3 Pa$ H_2/ $3 \cdot 10^3 Pa$ H_2O/ balance Ar (10ppm H_2S). Electrochemical impedance spectra were recorded using an Alpha-A High Performance Frequency Analyzer (Novocontrol Technologies, GER) in the frequency range of $1 \cdot 10^6 - 5 \cdot 10^{-2} Hz$. Analysis of impedance spectra was performed using the complex non-linear least squares fitting software ZView 3.2. Microscopic images were acquired with an Axio Imager M1m (Zeiss, AT) and processed with the software package AxioVision 4.8.2 SP3.

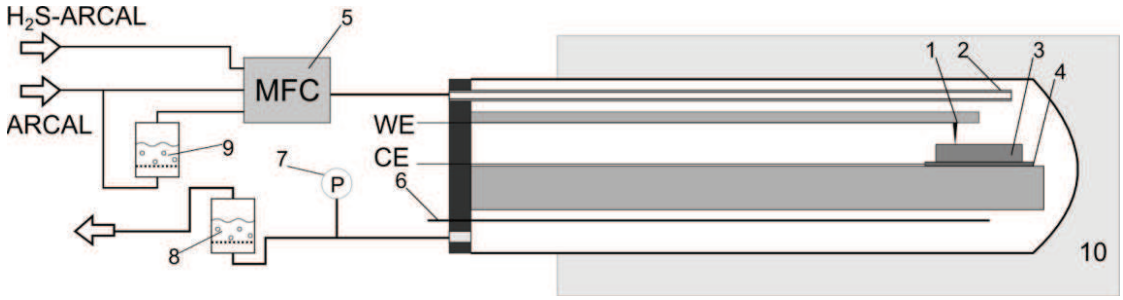

Figure 1. Basic construction of the used setup. 1 Contacting needle, 2 gas input, 3 sample, 4 CE current collector, 5 mass flow controller (MFC), 6 thermocouple, 7 pressure gauge, 8 $CuSO_4$-scrubber (only when H_2S is used), 9 humidifier, 10 furnace.

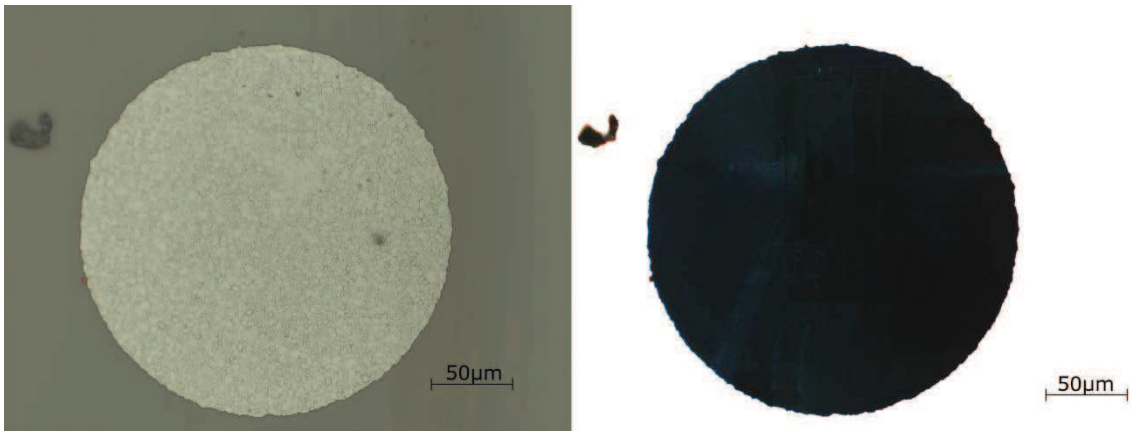

Figure 2. Reflected-light (lhs) and transmitted-light (rhs) bright-field image of a non-contacted circular microelectrode with a nominal diameter of 250µm after electrochemical testing for 45h at 750°C in $2.4 \cdot 10^3 Pa$ H_2/ $3 \cdot 10^3 Pa$ H_2O/ balance Ar. No porosity could be found.

Results and Discussion

Morphology, Geometric Properties

A microscopic image of a typical non-contacted circular microelectrode with a nominal diameter of 250 µm after electrochemical measurements is shown in figure 2. The figure shows that the electrode is dense and has corrugated edges. Since the grain size is in the µm-range the triple phase boundary length can be determined using such images. Image processing of 15 microelectrodes (5 electrodes on 3 samples each, data not shown) revealed a triple phase boundary length of $l_{TPB} = 924 \pm 54$ µm and an area of $A = (4.33 \pm 0.23) \cdot 10^4$ µm^2. The measured resistance and capacitance values are normalized to these average geometric values yielding length specific resistance (LSR) and area specific capacitance (C/A), respectively.

Impedance Spectra and Stability

A typical impedance spectrum of a microelectrode is shown in figure 3. The spectrum contains a high frequency x-axis intercept attributed to the spreading resistance of ion conduction in the electrolyte, which was modelled by a resistor (not included in the polarization resistance). The slightly depressed semicircle attributed to the electrode impedance was modeled by a resistor with a parallel constant phase element (CPE) (12). Therein the resistor represents the polarization resistance of the electrode and the CPE a non-ideal interfacial capacitance. True interface capacitances were calculated from the CPE's fitting parameters analogously to the work in Ref. (8).

A typical temporal evolution of the polarization resistance and interface capacitance is shown in figure 4. It can be seen that after an initial drift of the polarization resistance a relatively stable value is reached while the capacitance drift is small during the whole measurement series. In this series the final LSR-drift is ~0.1%/h while the final C/A-drift is ~0.04%/h. To accelerate stabilization processes an initial pretreatment at 800°C for 4h before measurements at 750°C (as suggested by Yao and Croiset) was introduced (6). The resulting drift of the polarization resistance can be seen below in the section 'sulfur poisoning'. Different microelectrodes prepared and measured by the above described method can therefore be compared to each other when the initial stabilization phase is sufficiently long (in this work >18h) and differences in LSR and C/A are much larger than the respective final drifts and differences in the geometric properties. The errors resulting from fitting the impedance spectrum to the very simple equivalent circuit (see fig. 3) will be neglected since the error is rather small and expected to have the same impact on all measurements.

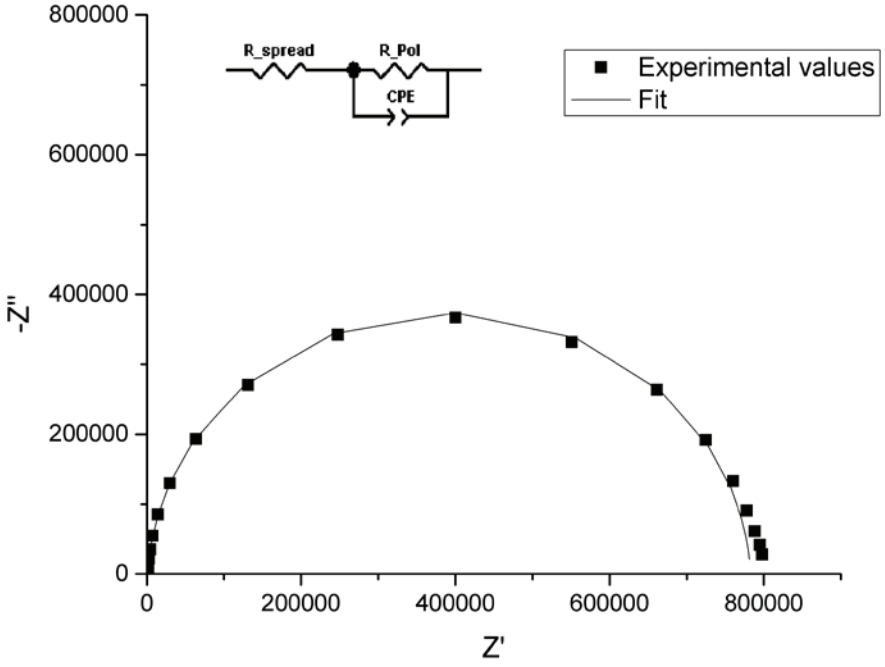

Figure 3. A typical impedance spectrum of a microelectrode measured at 750°C with fit from the shown equivalent circuit.

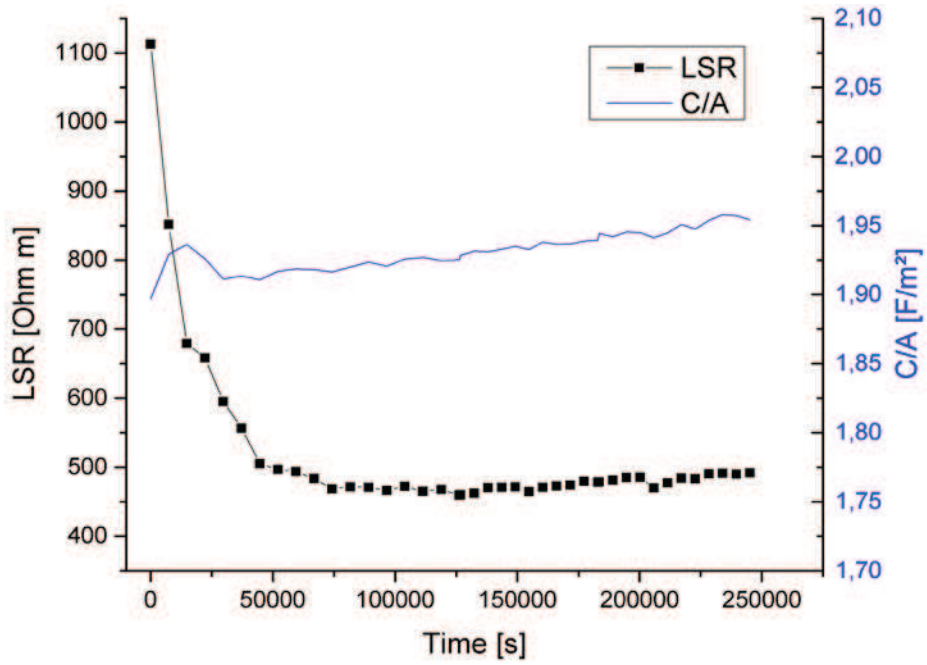

Figure 4. LSR and C/A change at 750°C in $2.4 \cdot 10^3 Pa$ H_2/ $3 \cdot 10^3 Pa$ H_2O/ balance Ar. After initial changes stable values can be obtained.

Substrate Orientation

As described in the previous section, measurements were conducted on electrodes deposited on different substrates – (100), (111), and polycrystalline YSZ. The resulting stable LSR and C/A values are shown in table 1 and illustrated in a scatter plot in figure 5. It can be seen that scattering between microelectrodes for both properties is much larger than errors described above. It is therefore safe to assume that a direct comparison of the data is possible without considering error propagation.

TABLE I. LSR and C/A values obtained from different substrates at 750°C by measuring different microelectrodes.

LSR [Ωm]			C/A [F/m²]		
111	**100**	**poly**	**111**	**100**	**poly**
813	907	299	1.38	1.67	2.77
1259	737	513	2.03	1.73	3.00
540	1479	2099	1.67	1.80	3.36
481			1.89		
1232			1.76		
1048			0.91		
2322			1.33		
2692			1.81		
547			1.35		
1812			1.49		
2255			1.46		

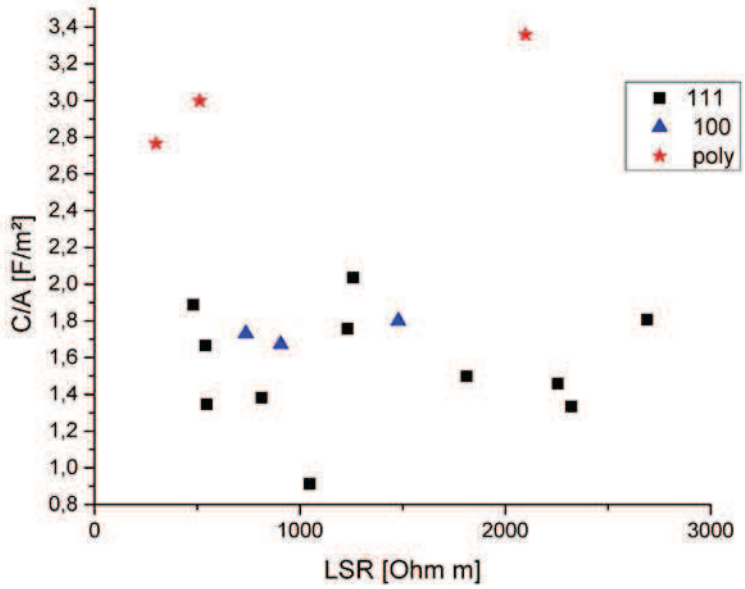

Figure 5. Scatter plot of LSR and C/A values shown in table I.

For statistical hypothesis testing, the significance level in this work will be set to $\alpha = 0.05$. The null-hypothesis of a given statistical test will therefore be rejected if the p-value of the test is smaller than the significance level. Since 2 sample t-tests require samples from normally distributed population, a Shapiro-Wilk-test was conducted for all available data sets (LSR and C/A values from each substrate orientation). All tests showed that normal distribution of the populations was not rejected (p-values not shown). The results of subsequent t-tests are summarized in table II. It can be seen that for all orientation combinations no significant differences were found for LSR values. Also, C/A values on the single crystalline substrates did not show significant differences. These results thus contradict the conclusions of Rao et al. (8). However, a significant difference between C/A values from single crystalline and polycrystalline substrates was found. This difference may be caused by different dopant concentrations, a rougher surface of the polycrystalline substrates increasing the actual interface area or a different contamination of the electrode/electrolyte interface. Giving a definite explanation for this phenomenon is, however, beyond the scope of this study.

TABLE II. p-values for 2-sample t-tests comparing average LSR- and C/A-values from different orientations. The tests gave the same conclusion regardless of equal variance or unequal variance (Welch-corrected values).

		LSR		C/A	
		100	**poly**	**100**	**poly**
111	Equal Variance	0.51	0.48	0.36	9.8E-6
	Welch-corrected	0.36	0.57	0.10	0.0032
100	Equal Variance	-	0.91	-	0.0018
	Welch-corrected	-	0.91	-	0.014

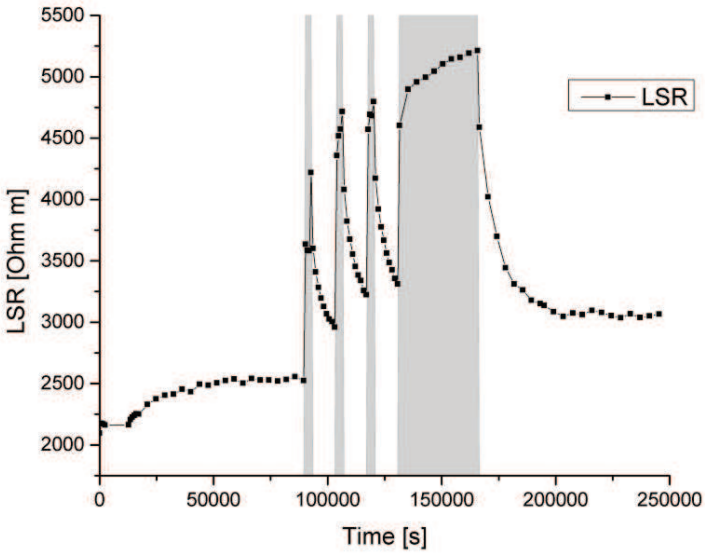

Figure 6. LSR data obtained in a sulfur poisoning experiment on a Ni/(111)YSZ microelectrode. H_2S was added to the feed during the timespans highlighted in gray. A small high frequency feature in the impedance spectrum (<2 % of total resistance) attributed to the counter electrode was not included in the LSR.

Sulfur Poisoning

The effect of H_2S on the polarization resistance was examined on a (111)-oriented YSZ substrate by initially stabilizing the microelectrode (see sections above), then adding H_2S to the gas feed and finally removing H_2S to observe regeneration behavior. Such a measurement series is depicted in figure 6. It can be seen that after stabilization of the polarization resistance a sharp increase is found after addition of H_2S which is slowly partially reversed upon removal of H_2S in the feed. This behavior is qualitatively coherent with findings on Ni/YSZ cermet electrodes (9).

Conclusions

In this study, a method for preparation of electrochemically stable Ni microelectrodes on YSZ was developed. It was found necessary to wait for polarization resistance stabilization to obtain results that allowed comparison of different microelectrodes. Due to the strong scattering of LSR and C/A values errors from other sources like residual drift or geometry deviations could safely be ignored.

Statistical analysis of LSR and C/A values ($\alpha = 0.05$) obtained from microelectrodes on different substrates showed no significant differences in LSR values for any tested substrate combination. For C/A values no significant difference between the (100) and (111)YSZ substrate was found, but the polycrystalline substrate showed a significantly higher capacitance compared to the single crystalline substrates. It can therefore be concluded that direct comparison of literature data obtained from different substrates is possible.

Sulfur poisoning experiments on microelectrodes yielded qualitatively equivalent results to analog experiments on Ni/YSZ cermet electrodes. These results on microelectrodes, however, directly quantify the changes in triple phase boundary kinetics and are therefore valuable input for future sulfur poisoning modeling of cermet electrodes.

Acknowledgements

The financial support by the Austrian Federal Ministry of Science, Research and Economy and the National Foundation for Research, Technology and Development is gratefully acknowledged.

References

1. W. G. Bessler, M. Vogler, H. Stormer, D. Gerthsen, A. Utz, A. Weber and E. Ivers-Tiffee, *Physical Chemistry Chemical Physics*, **12**, 13888 (2010).
2. A. Ehn, J. Høgh, M. Graczyk, K. Norrman, L. Montelius, M. Linne and M. Mogensen, *Journal of The Electrochemical Society*, **157**, B1588 (2010).
3. K. V. Hansen, K. Norrman and M. Mogensen, *Journal of The Electrochemical Society*, **151**, A1436 (2004).
4. A. Utz, K. V. Hansen, K. Norrman, E. Ivers-Tiffée and M. Mogensen, *Solid State Ionics*, **183**, 60 (2011).
5. W. Yao and E. Croiset, *Journal of Power Sources*, **248**, 777 (2014).
6. W. Yao and E. Croiset, *Journal of Power Sources*, **226**, 162 (2013).
7. A. Utz, H. Störmer, A. Leonide, A. Weber and E. Ivers-Tiffée, *Journal of The Electrochemical Society*, **157**, B920 (2010).
8. M. V. Rao, J. Fleig, M. Zinkevich and F. Aldinger, *Solid State Ionics*, **181**, 1170 (2010).
9. M. Gong, X. Liu, J. Trembly and C. Johnson, *Journal of Power Sources*, **168**, 289 (2007).
10. D. S. Monder and K. Karan, *ECS Transactions*, **35**, 977 (2011).
11. T. M. Huber, A. K. Opitz, M. Kubicek, H. Hutter and J. Fleig, *Solid State Ionics*, **268, Part A**, 82 (2014).
12. F. S. Baumann, J. Fleig, H.-U. Habermeier and J. Maier, *Solid State Ionics*, **177**, 1071 (2006).